A. Delannoy †
(Onera)
P. Gondot
(Airbus)

E-mail: pascal.gondot@airbus.com

Airborne Measurements of the Charge of Precipitating Particles Related to Radar Reflectivity and Temperature within two Different Convective Clouds

Simultaneous ground based radar reflectivity measurements and airborne electric parameters (electrostatic field and charged particles) are presented. They are used to investigate the charging processes acting in convective cells. Within the two thunderclouds presented in this work, both signs are found on large hydrometeors. It is shown that negative particle charging exists at high levels in classical vertically developed cells. There is some evidence that positive charging of precipitating particles is occurring in the lower parts of the clouds.

Introduction

The charge separation, which occurs when an ice particle collides with a graupel, has received increased attention over the last few years, as a possible mechanism for the electrification of thunderstorms. Laboratory studies following the pioneering work of Reynolds et al. (1957)[1] have provided evidence for a viable ice collisional charging mechanism. The works of Takahashi (1978) [2], Jayaratne et al. (1983) [3] and, more recently, Emersic and Saunders, (2010) [4] pointed to the dependence of sign and magnitude of charging efficiency on temperature, cloud liquid water content (LWC), particle size and velocity. Note: many papers on this topic have been published since 1983 - this 2010 paper includes references to most of them.

An important general result of these experiments is the existence of two domains for graupel charging: positive charging at a higher temperature and higher LWC, and negative charging at a lower temperature and LWC. Under natural realistic conditions, the transition between these two domains depends on cloud water content and could occur at temperatures typically between -20° C and -10° C. Note: both studies give a range of charge sign reversal temperatures and liquid water contents - and we now know that this depends on supersaturation too.

Aircraft observations of convective clouds reported evidence of the association of electric charge with ice particles. Generally, the highest charge densities are coincident with regions of high graupel concentration (Gardiner et al., 1985) [5]. Dye et al. (1988)[6] observed two electrified regions during initial thunderstorm electrification. In both regions, supercooled water and ice particles, including graupel, were present and solid particle concentrations, sizes, and collision rates were at a relative maximum. A great number of observations were related to the negative charge center of the cloud, but in all cases particle charge measurements reported the presence of both signs at the same location.

Thus, the combined information from laboratory and *in-situ* measurements suggests that charge generation is probably associated with ice particle collisions. From a schematic point of view and according to the classical picture, the smallest positively charged ice particles, ice crystals, are carried by updrafts to the top of the cloud and the largest negatively charged riming particles, like graupel grow near the -15° C level, thus developing the classical thunderstorm electrostatic dipole.

Our purpose in this paper is to report observations, which could be discussed and analyzed within the context of particle charging in thunderstorms. During Summer 1984, in the South-West of France, *in-situ* measurements of electrostatic field, precipitation charge and size were collected in two quite different convective situations. On June 6th, an exceptional meteorological situation was observed by an instrumented aircraft and by a meteorological radar system. In order to point out the main electrical features of these convective cells, it seems interesting to compare observations on June 6th with a more classical case encountered a few days later, on June 24th.

The most important feature pointed out in this paper concerns electrical parameters, precipitation charge measurement in particular. The net charge carried by precipitation observed in the same range of flying levels was of opposite sign in the two kinds of convective cells. A preliminary report of these observations was made by Delannoy et al. (1988)[9].

The airborne observations described here were made during the Landes-Fronts '84 experimental program, which covered a large set of complementary measurements, including a ground-based network, in order to be able to analyses frontal or isolated convective cells. More details were reported in several publications, for instance, see Laroche et al. (1985) [7] or Laroche et al. (1986) [8].

Among the experimental capabilities was a C160 Transall aircraft, which was first dedicated to triggering lightning and recording electromagnetic parameters, but was also used to make electrical and microphysical basic measurements in and around the clouds. The aircraft was fitted with several types of sensors: a network of five field-mills, a complete set of PMS (Particle Measuring Sensor) probes and an induction ring to measure particle charges. A short account of this last sensor is presented in box 1. The locations of the main sensors on the aircraft are reported in box 2.

Many flights of the Transall were made in conjunction with radar reflectivity measurements. The aircraft location was determined with the inertial system rechecked with a tracking radar, to give an accuracy of about 100 meters on the aircraft trajectory. This enables us to make good spatial correlations between *in-situ* measurements and radar reflectivity data.

Comparison of data obtained on June 6th, during flight A and on June 24th, during flight B

Figure 1b presents radar reflectivity obtained during flight B. It indicates that the convective cells in the scanning region have a strong precipitation core (more than 40 dBz) with a vertical extent of 7 kilometers. Such clouds were currently observed during the entire campaign.

On the other hand, the convective situation encountered on June 6th (flight A) was exceptional: a thick layer of cirrus clouds were visually observed above the site between 5 and 7 kilometers. The vertical convective motion was stopped below this level. Typical reflectivity obtained during this flight is presented in figure 1a. From the vertical cross section, it can be seen that the precipitation core was entirely below the 4 kilometer level. Precipitating particles were all below the -20° C isotherm. All of the cells scanned during this flight exhibited the same characteristics.

In figure 2, we present charge measurements collected during these two flights. One must keep in mind that the main goal of the campaign was to trigger lightning by the aircraft itself. This implied that the clouds were crossed as frequently as possible, the flight path being determined by electric field measurements. Due to aircraft limitations, most of the penetrations took place between the 2 km and 5 km levels. The cells identified in figures 1a and 1b were crossed several times at several levels in this interval. Other similar cells in their vicinity were sampled too.

For each pass through the cloud, a histogram shows all of the charged particles detected by the induction ring. The histogram is made up of 32 classes, 16 for each sign. The width of every class is $15\ pC$. The two first classes $(|q| < 15\ pC)$ are empty because of the choice of a threshold value of $15\ pC$ (see box 1). The two highest classes $(|q| > 225\ pC)$ are incremented even if the measured charge is greater than $240\ pC$: in such cases, the amplifier is saturated and the charge value is not correctly measured, but we are interested in the counting of highly charged particles, which is always normally operating.

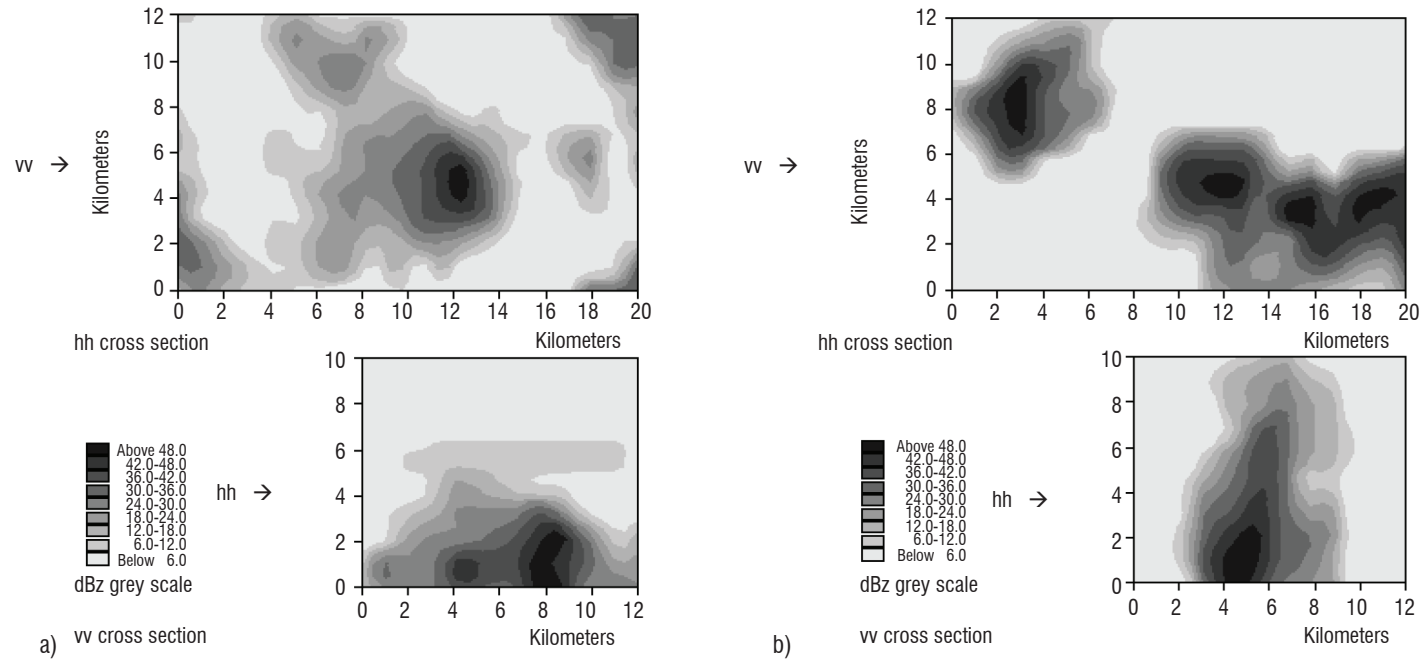

Figure 1- Radar reflectivity cross-sections obtained during flight A and flight B

Box 1 - Measurements of electric charges carried by large hydrometeors

The electric charge of precipitating particles is measured using an induction ring (FARADAY cylinder), which is described in figure B1. The sensing electrode is dimensioned so as to contain no more than one particle at a time. It is mainly concerned by the same class of particles as the PMS 2 DP probe. The volume of cloudy air sampled at a true airspeed of 100 m/s is around 70 l/s.

Special care is taken to avoid corona discharges from leading edges and the sensing part of the device is shielded and insulated. The shape of the guard rings and of the electrode is conical, to minimize collision efficiency between precipitation particles and the inner side of the sensor.

a)

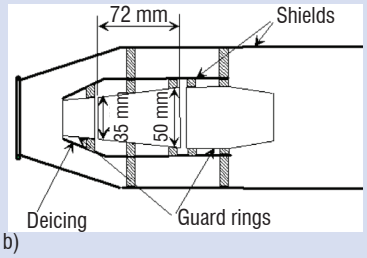

b)

Figure B1-1
a) The induction ring on the left pod, under a PMS probe
b) dimensions of the sensing electrode

The sensor is located on a pod under the wing in the same vertical plane as the propeller, at about 10m from it. (see figure B2 - 1)

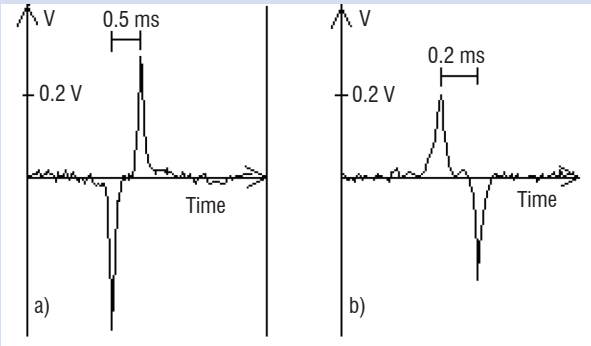

Figure B1-2 Signals obtained with a positive (a) and a negative (b) particle

The detector electronics are made with low noise and high gain amplifiers. Typical signals of both signs are shown in figure B1-2. If the current peak value is greater than a threshold value S, the signal enters a process unit. To be accepted, the pulses generated by a particle passing through the device must be symmetric (the extremes are inverted when the particle goes in and out the induction ring without colliding) and the time interval between the two sharp extremes must be equal to the length of the electrode (72 mm) divided by the particle relative velocity, which is not very different of the airspeed.

If one of these conditions fails, the pulse is rejected. Counting of such events is performed. If both conditions are true, it is assumed that a single particle has penetrated the device and exited without colliding. Spurious signals are found to be less than 5% of the acquired signals.

When a pulse is valid, the charge carried by the particle is calculated by the formula:

$$q = \alpha . \Delta i . \Delta t$$

where:
Δi is the difference of intensity between two extremes values
Δt is the time interval between two peak values coefficient deduced from laboratory calibrations.

According to its charge value, the particle enters under 32 classes (16 for each sign).The full process lasts for 4ms and is initialized at each time a “significantly charged” particle enters the probe bin. The error rate for classifying is 10%. However, if there are more than 3 valid events per liter (less than 4ms between two consecutive events), some of them are ignored by the processing system and counting is underestimated. The choice of a threshold value is a convenient way of limiting the number of events to be taken into account by the processing unit. With $S = 15\ pC$, the maximum number of detected charges is about 100 per second for the entire campaign, that is, less than two “significantly charged” particles per liter.

Box 2 -Electric field measurements on the aircraft

Electric field measurements are made at five locations on the fuselage. The sensors are of the field-mill type. Their location is displayed in figure B2-1b. Laboratory calibrations were made on a scale model aircraft, to assess the amplification coefficients resulting from the curvature of the fuselage.

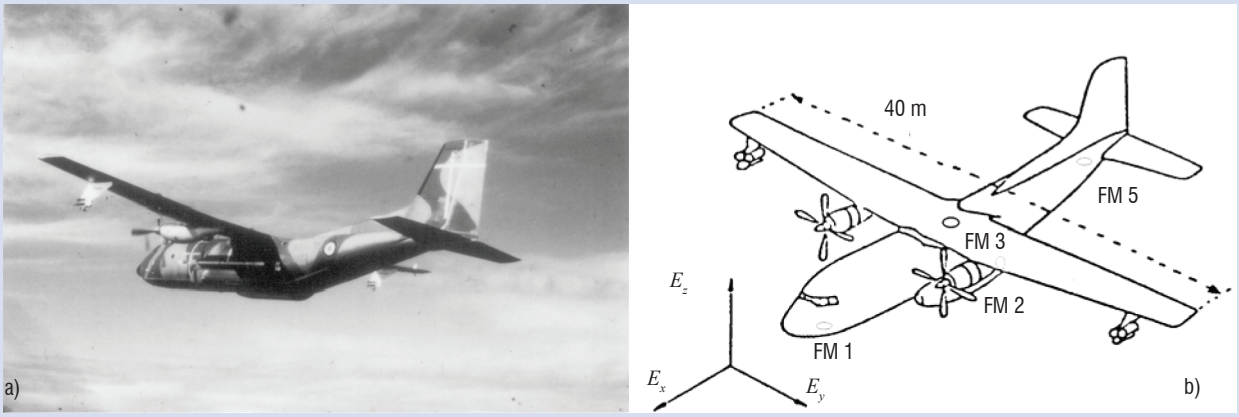

Figure B2- 1 The instrumented C160 aircraft end the locations of its five field-mill sensors

These coefficients can also be deduced by numeric integration of Poisson's equation on a modeled structure. The three atmospheric electric field components and the electrostatic potential of the aircraft are retrieved from the five measured signals, by means of a least square method (see Laroche et al., 1985)[7].

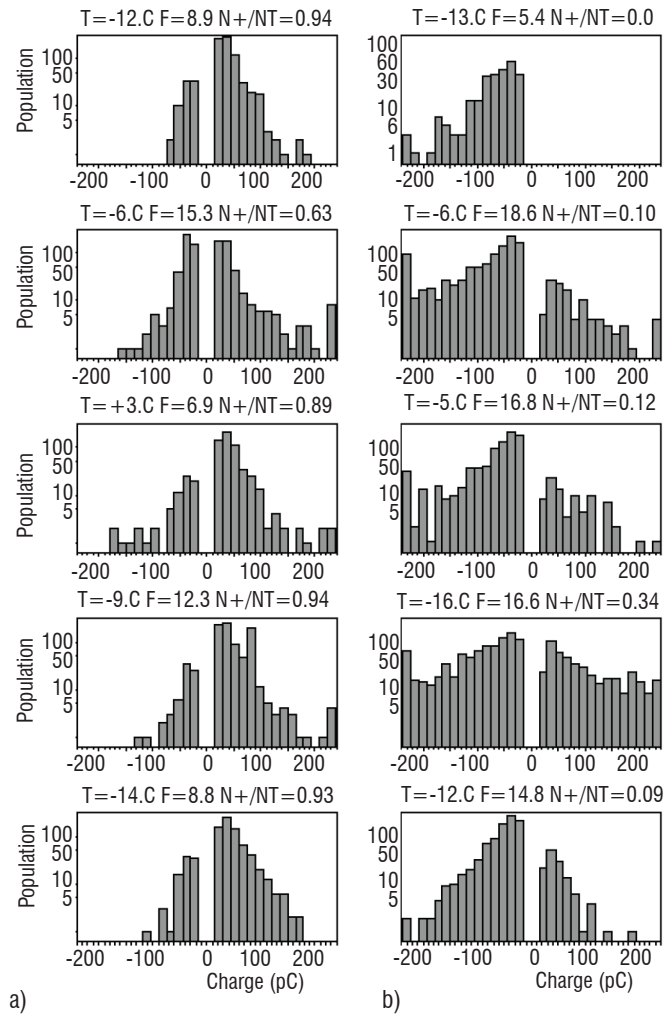

Figure 2 - Histograms of charges recorded during flight A and flight B

The histograms presented in figure 2 have been chosen from a larger set (approximately 20 penetrations per flight) to illustrate the charge distribution at different levels in two different meteorological situations. The duration Dt of each pass through the cloud is variable, depending on the in-cloud path of the aircraft and its velocity. Knowing the total number NT of charged particles encountered during a penetration, we define an average rate F of charged particles per second $(F=NT/Dt)$. The ratio $N+/NT$ indicates the proportion of positively detected charged elements. The histograms collected during flight A are referenced in column a (flight B, in column b). The average density of detected charged particles can be deduced from F and from the aircraft velocity and the collecting surface of the induction ring:

$$D = K^{-1}.F$$

with

$$K = Vp.\,Se$$

D is the average density in m^{-3}, Vp is the aircraft velocity in m/s and Se is the collecting surface of the induction ring in m^2. For flight A and B, K is close to 0.07.

We observe that, in most cases, positive and negative charges are both detected simultaneously, located at a given altitude in the range of our flying levels. Temperature measurements indicate that these levels are between the -16° C and +3° C isotherms. Obviously, most of the charges are positive in the data obtained during flight A; they are negative for flight B, although they were sampled within the same range of altitudes.

The population of the classes decreases when the absolute value of the corresponding charge increases, but the highest classes $(|q| > 225\,pC)$ often contain a high number of particles. Close examination of the data indicates that the filling up of those highest classes is always achieved in a few consecutive seconds, that is, during the crossing of a n unique narrow vertical layer.

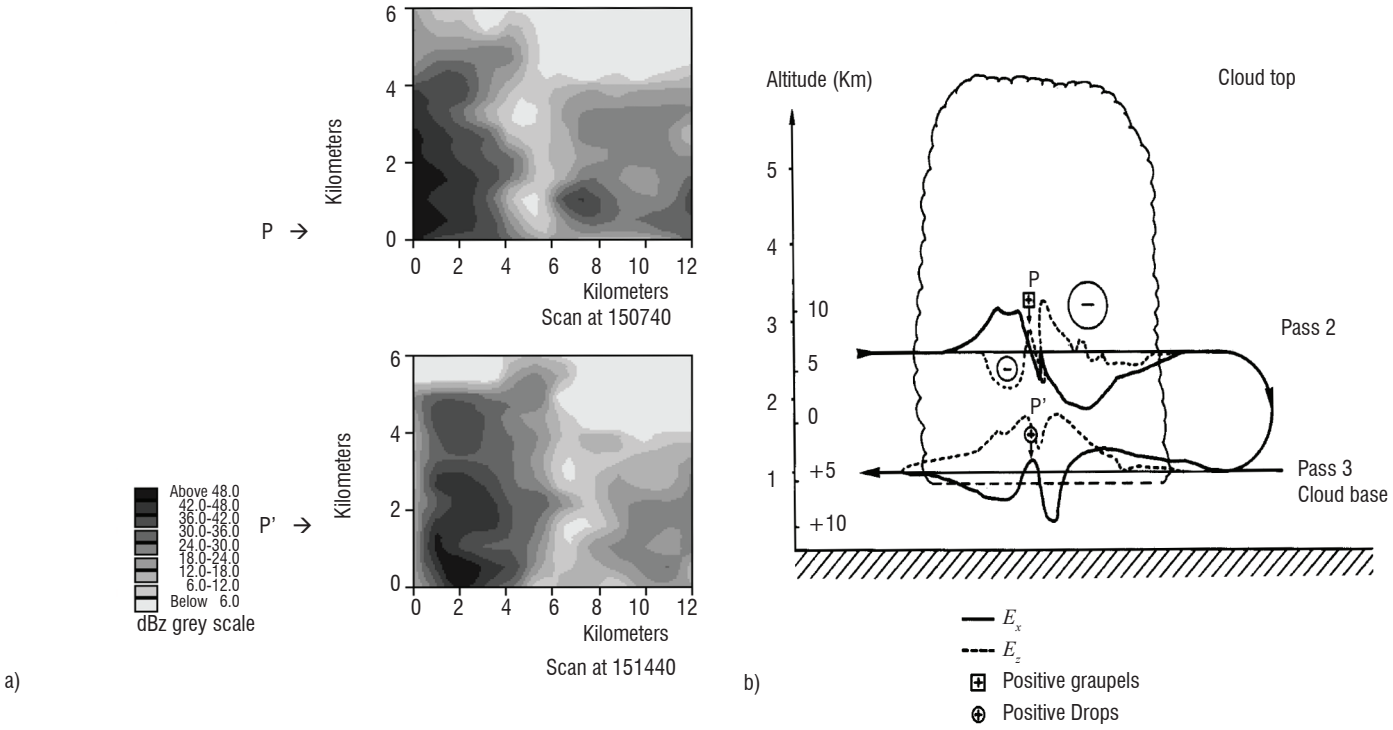

Figure 3 – Two scans and two flight paths through the same cell. a)Vertical scans of the cell, with indication of the two penetrating levels. b) Vertical cross-section in the cloud reference frame

The mean value of F for the 5 data sets of flight A is $F_A = 10 \pm 3$. The corresponding value for flight B is $F_B = 14 \pm 5$. The mean flow of charged precipitation through the induction ring is not so different from one situation to the other. It may be noticed that we detected more natural lightning during flight B than during flight A. Nevertheless, the intensity of the radar reflectivity, the total number of charged particles and the absolute value of the charges carried by precipitation are within the same order of magnitude for both of the kinds of cells under examination. They differ mainly by the vertical extent of their 50 dBz cores, by the temperature level reached by their tops, and by the dominant sign of their charged precipitating particles. For flight A the $N+/NT$ ratio lies between 0.63 and 0.94; for flight B , between 0.0 and 0.34.

Comparison of data obtained in two consecutive crossing of a single cell during flight A

We now present data from a cell which was penetrated during flight A at 150830 UT. The altitude of the aircraft was around 2700 m (level *P* in figure 3a, $T = -6° C$).The corresponding histogram of charges is presented in figure 2a. At this time, the cell was just entering the scanning region of the radar. As can be seen in figure 3a, the precipitation core (more than 40 dBz) reaches the 4 km level. At 15:15:00 UT, the cell was crossed again at a lower flying level (level P' in figure 3a, 1600 m, $T = +3° C$, corresponding histogram in figure 2a). From figure 3, we observe that the cell has moved between two consecutive radar scans. The two vertical planes of the reflectivity cross section are chosen according to the horizontal velocity of the cell. The top of the 40 dBz core is now under the 3 km level. Referring to the reflectivity data and to the tracking of the aircraft it can be established that this pass is just below the preceding one in the cloud frame of reference (figure 3b). The ratio $N+/NT$ is 0.63 for the first pass and 0.89 for the second one. Thus, while the cell is descending, the flying level of the aircraft is lowering too and there are fewer negatively charged particles. The distribution of positive charges is not clearly different from figure 2a ($T = -6° C$ and $T = +3° C$) when integrated over the whole path through the cloud.

In figure 4, these two consecutive penetrations are examined in more detail. The use of electrostatic data allowed us to identify different zones, which can be analyzed with a better spatial resolution. In this paper, we do not try to calculate charge distributions, which would give rise to the observed electric field components. Nevertheless, looking at the E_x component in figure 4a, we observe that it has a smooth shape on which an event (marked P) identified by the important positive slope of E_x is superimposed. This happens at 15:09:08 UT; the dimension of this zone along the trajectory of the aircraft is about 300 m. At this time, the aircraft is flying through a high reflectivity region. Graupel with sizes of up to 3 mm are sampled by the 2 DP probe.

In the lower part of figure 4a, the time interval during which the higher classes of the histogram are incremented, is marked. Event P occurs during this time. Only 8 particles carrying a charge greater than *200 pC* are detected by the induction ring.

E_x and E_z components are affected by event P in such a way that it is coherent to localize a region of positive charge in this part of the cloud. Triboelectric charging by impact of solid particles usually consists in negative charging of the aircraft and in a decrease in its electrical potential toward high negative value. This is observed in our case, when the aircraft fly through this region characterized by a high concentration of large and solid precipitating particles.

Data sampled by PMS 2DP probe during the P event 6400 μm

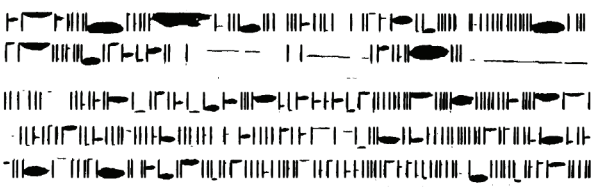

Data sampled by PMS 2DP probe during the P' event 6400 μm

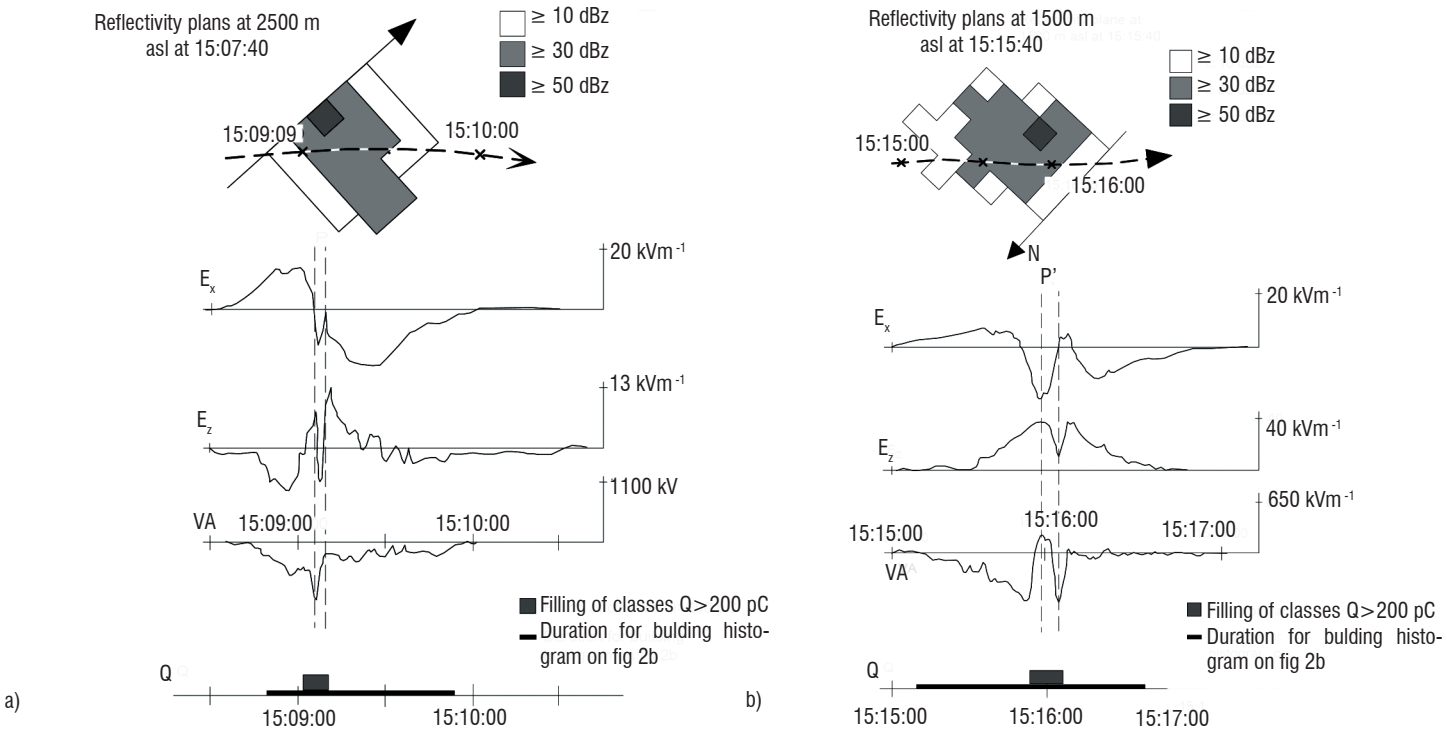

Figure 4 - Detailed data obtained during two flight legs: 2DP PMS, horizontal cross-section of radar reflectivity, electrostatic components E_x, E_z and potential, duration of the collection of charged hydrometeors.

There was no simultaneous measurement of the size and of the charge of an individual particle, the volumes sampled by the induction ring and by the 2 DP PMS being different. Thus, we may summarize what we have learnt on region P in the following manner: a narrow region of positive charge, with large precipitating hydrometeors, including few elements carrying positive charge higher than anywhere else along the trajectory.

Data obtained during the second crossing is displayed in figure 4b. We can notice that in a similar manner, an event marked P' characterized by a strong positive slope is superimposed on a regular evolution of E_x component. The vertical component E_z decreases and then increases again, while the slope of E_x remains positive: a region of positive charge is entered when E_x reaches its minimum value at 15:15:58 UT; its horizontal extension along the path is about 800 meters.

Event P' is encountered roughly 1000 meters below event P. It can be seen on data from the $2\ DP$ probe, that large solid particles are sampled with the addition of some large liquid drops. By splashing on the device, they produce a thin trail visible on the frame at the top of figure 4b. The triboelectric effect is inverted from event P to P': the aircraft's potential is increasing during the crossing of this region. This may be the result of crossing a liquid precipitation zone, as the splashing of large water drop produces negatively charged droplets, which are transported by air flow, the impact process charging the aircraft positively.

Simultaneously, the induction ring detects highly charged elements; the time during which the higher positive classes are filled is plotted on the lower part of figure 4b. Event P' appears to be similar to event P, with a larger extension along the aircraft's path. The reflectivity echoes and the precipitation rate are of the same order of magnitude for both passes, but the horizontal variations of electrostatic field's components are slower during the second crossing. This may result from the lower flying level and from the subsidence of the explored cell, as it is displayed on figure 3.

For a better comparison between the charge distribution during event P and P', it is useful to build histograms of the same duration including the two intervals of filling of the higher classes. These are presented in figure 5. The total number of charged particles detected in 16 seconds decreases from 380 to 180 and the ratio $N+/NT$ increases from 0.60 to 0.92. The number of negatively charged particles in the two corresponding regions defined by a positive slope of Ex undergoes a sharp drop between the two temperature levels $T=-6°\ C$ and $T=+3°\ C$, while the precipitation core of the cell is descending.

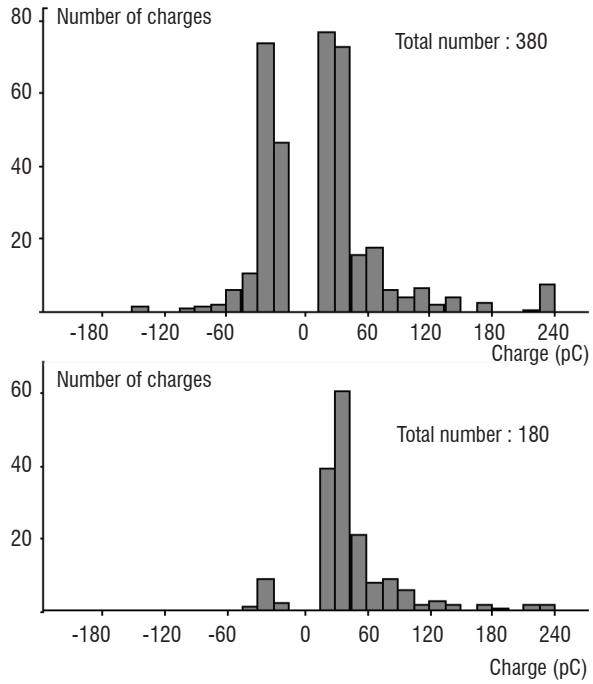

Figure 5 - Histograms collected during events *P* and *P'*

A concluding remark may be that most of the positively charged particles in this core carry less than $100\ pC$, but a narrow region exists with a noticeable vertical extension where few highly charged elements are found.

Concluding discussion

The charge acquired by a particle is not defined by the location at which it is sampled. It reflects its history in the cloud and depends on its travel during its entire life. Everywhere in the cells explored during flight A and B, we find the simultaneous presence of positive and negative charges on particles, but the higher the top of the cloud is, the more numerous negatively charged elements are at every level between 2 km and 5 km.

Cells of flight A and B differ mostly by the temperature of their top, the precipitation rates being not so different. For all of the cells explored during flight A, $N+/NT$ lies between 0.63 and 0.94, indicating that at all flying levels negatively charged particles detected are less numerous than positive ones. Conversely, during flight B $N+/NT$ is less than 0.34. Following our observations, a precipitation core confined in a range of temperatures warmer than -20° C seems to result in an important deficit in the negative population of the lower part of the cloud. The level at which precipitating particles appear may determine the sign of their initial charging, the colder tops of clouds being likely to promote negative charging.

In addition, negatively charged precipitation particles are less and less numerous when we sample particles at warmer levels, while the top of the cell is descending (flight A). It indicates that a positive charging mechanism is acting on precipitation in the range of altitudes of our explorations. This mechanism increases the ratio $N+/NT$: focusing on events P and P' or considering the whole passes at two flying levels, this positive charging acting in the lower part of the cell increases $N+/NT$ from 0.6 to 0.9 when the temperature increases from -6° C to +3° C. No values smaller than 0.6 are found for this ratio during flight A. This may be related to the little vertical extension of the upper region in which a negative charging may be efficient. In the regions that were explored during flight B, positive charging is working against the negative one, which is supposed to have worked at levels above the aircraft's passes. The histograms in figure 2b are obtained from crossings of different cells at different stages of their evolution, so they are not suitable for comparison between them. However, since we find much more negative charges than during flight A at the same altitude, we may conclude that the vertical extension of the negative charging zone is large enough to build an important population of negatively charged precipitation. The action of the positive charging all along the travel of the particles in the warmer part of the clouds is not sufficient to shift most of the observed charges to positive values: $N+/NT$ remains relatively low.

Because we have no direct measurements of the particle charge flux (which is the main point of interest in terms of the microphysical process), our data must be used with some assumptions, if we want to relate it to laboratory experiments. These assumptions may be rejected, but taking into account that we had the opportunity to observe an exceptional electrified cloud warmer than -20° C, these observations build a consistent description of a natural medium where a charging process depending on temperature is likely to act on solid precipitating particles. They argue for a reversal temperature. This charge-sign inversion occurs at altitudes higher than our flying levels, since positive charges are detected everywhere (with one exception, see figure 2b, T=-13° C). Negative charging occurs in the colder part of typical cells and if this upper part is not very tall, negatively charged particles at lower levels are fewer. Furthermore, these observations give us the opportunity to indirectly detect the positive charging acting in this lower part. Thus, the two distinct regions for charging pointed out by laboratory experiments seem to be efficient in natural conditions, and the whole microphysical process may be of major importance for the electrification of convective clouds ■

References

[1] S.E. REYNOLDS, M. BROOK and M.F. GOURLEY - *Thunderstorm Charge Separation.* J. Meteo., 14, 426-436, 1957

[2] T. TAKAHASHI - *Riming Electrification as a Charge Separation* . J. Atmos. Sci., 35, 1536-1548, 1978

[3] E.R. JAYARATNE, C.P.R. SAUNDERS and J. HALLETT - *Laboratory Studies of the Charging of Soft Hail During Ice Crystal Interactions.* Q. J. R. Meteo. Soc., 109, 609-630, 1983

[4] C. EMERSIC and C.P.R. SAUNDERS - *Further Laboratory Investigations into the Relative Diffusional Growth Rate Theory of Thunderstorm Electrification.* Atmos. Res. 98, 327-340, 2010

[5] B. GARDINER, D. LAMB, R.L. PITTER and J. HALLETT - *Measurements of Initial Electric Field and Ice Particle Charges in Montana Summer Thunderstorm.* J. Geophys. Res., 90, 6079-6086, 1985

[6] J. E. DYE, J. J. JONES, W. P. WINN, T. A. CERNI, B. GARDINER, D. LAMB, R. L. PITTER, J. HALLETT and C. P. R. SAUNDERS - *Early Electrification and Precipitation Development in a Small Isolated Montana Cumulonimbus*. J. Geophys. Res., 91, 1231-1247, 1986

[7] P. LAROCHE, M. DILL, J. F. GAYET and M. FRIEDLANDER - *In-Flight Thunderstorm Environmental Measurements During the Landes 84 Campaign.* 10th Int. Aerospace and Ground Conf. on Lightning and Static Electricity, PARIS, 1985

[8] P. LAROCHE, A. DELANNOY, P. GONDOT, F. HELLOCO and J. F. GAYET - *Airborne Observation of Small Scale Fluctuation of Microphysical Dynamic and Electrical Properties in Convective Clouds.* 23rd Conf. on Radar Meteorology and Cloud Physics, SNOWMASS, COLORADO, 1986

[9] A. DELANNOY, P. GONDOT, F. HELLOCO and P. LAROCHE - *Airborne Precipitation Charge Measurement Related to Local Electrostatic Field and Temperature.* 8th Int. Conf. on Atmospheric Electricity, UPSSALA, 1988

Acronyms

PMS (Particle Measuring Sensor)

AUTHORS

Alain Delannoy † *(1951-2012*) received a PhD in Atmospheric Physic from University Paris 6 in 1979. He joined Onera in 1980 and was engaged in research on Atmospheric Electricity, Cloud microphysic and Physic of Lightning. His interest focused on in situ electrical measurements in cloud for what he setup specific instrumentations. He was engaged in lightning strike experiment on aircraft. Alain Delannoy was author and co-author of numerous articles and reports on Atmospheric Electricity and Lightning.

Pascal Gondot received a PhD in Atmospheric physic from University Paris 6 in 1985 and a PhD in Physical Meteorology from University of Clermont-Ferrand in 1988. After 5 years at Onera he joined the EADS Corporate Research Centre (Innovation Works) where he became the head of EMC and Lightning Department and EADS Senior Expert in Hardening of systems. He is now in charge of the development of R&T Partnerships and Co-operations for Airbus Operation SAS.